Research on Comprehensive Calibration Techniques for Single-axis Rotational Inertial Navigation System

CHENG Jianhua[1,2], CHEN Daidai[1], Rene Jr. Landry[2], GUAN Dongxue[1,2] and WANG Xiuzhi[3]

1. College of Automation, Harbin Engineering University, Harbin 150001, China

E-mail: ins_cheng@163.com, ins_dai@163.com, dongxueguan@hotmail.com

2. Ecole de Technologie Superieure, Université du Québec, Montréal H3C 1K3, Canada

E-mail: rene.landry@etsmtl.ca

3. Tianjin Long March Launch Vehicle Manufacturing Co.,Ltd, Tianjin 300462, China
E-mail: wangxiuzhi_2011@163.com

Abstract: For long-time operation applications based on single-axis rotation inertial navigation system (SRINS), the estimation and compensation of gyroscope's constant drift along the rotational axis in comprehensive calibration is the most important problem. In this paper, a novel comprehensive calibration method for SRINS is presented. During this process, SRINS is operating in the outer level damping mode. Kalman filter has been designed based on the SRINS model with the damping network. The velocity and position provided by differential GPS (DGPS) are introduced as reference information for the estimation of rotational axis gyroscope drift. For stationary scenario, the observability degree of system states are given by an observability analysis based on singular value decomposition. The validity of this method is confirmed by simulations. The influence of linear accelerated motion on the estimation of drift is obtained.

Key Words: SINS, rotation modulation, horizontal damping, gyroscope drift

1 Introduction

Improvements in optical strapdown inertial navigation system (SINS) technology have made the optical SINS available in the high precision navigator [1]. Because of the random errors of inertial sensors, it is difficult to maintain a high performance of positioning after long-time operation. There are two conventional approaches to solving this problem: a) modifying inertial sensors; b) utilizing compensation technologies.

Novel high accuracy inertial sensors have been always one of the optimal solutions for improving the performance of SINS. However, there are a set of drawbacks for this method such as high cost and long development cycle.

With appropriate cost and obvious improvement on system performance, many system compensation technologies have been actively developed and widely used for SINS. The techniques of rotational modulation and calibration are the two most commonly used. By the implementing rotational mechanism, the rotation modulation could achieve an auto-compensation for the constant errors of the sensors which are mounted in the vertical plane of the rotation axis [2]. Consequently, the influence of sensor errors on navigation is asymptotically restrained and the long-term performance of SINS is enhanced. For instance, the condition with the same sensors being adopted, MK39 Mod3C which has employed single-axis rotational modulation scheme exhibits a positioning accuracy of 1nm/24h, while MK39 Mod3A's accuracy is 1nm/8h without rotation. However, there are only 0.2 million dollars additional cost [3].

For some special applications such as submarine and lager surface ships, super-long efficient working time is demanded. Therefore, calibration by introducing outside accurate reference information might be the only solution for prolonging the effective working time of SINS. The basic contents of calibration include resetting parameters, estimating and compensating sensor constant errors which are time-varying with an extreme small value and need to be countervailed in the navigation calculation. After an effective compensation, most of system errors approach to zeroes so that the SINS errors grow with lower speeds in the following navigation cycle [4].

As the single-axis rotational modulation scheme is applied, all the sensor constant errors are modulated except the drift error along rotation axis. As a result, the gyroscope constant drift becomes the main error source causing the accumulation of system positioning errors. Hence, the key to comprehensive calibration for SRINS is to obtain and compensate the gyroscope error along rotation axis [5].

In this paper, a novel comprehensive calibration approach for azimuth axis rotation of SINS is presented. The error model of SRINS concerning the level damping network has been established with an appropriate system time constant to accommodate the long-term filtering requirement. The Kalman filter for comprehensive calibration is designed. The velocity and position provided by DGPS are taken as reference information in order to estimate the drift of rotational axis. Observability analysis of this calibration system is conducted to predict the potential performance of this scheme. Validity of this method is proved by simulations. Results show that the drift can be accurately

*This work is supported by National Natural Science Foundation of China under Grant 61374007, 61104036 and 61273081, and the Fundamental Research Funds for the Central Universities under the grant of HEUCFX41309 and HEUCF0414.

estimated, and the influences of linear maneuver on calibration are analyzed.

2 Error Model of SRINS with Level Damping

2.1 Error Model of SRINS Rotating in Azimuth Axis

According to the rotation, the system matrix is sinusoidally varying with respect to the azimuth axis. The system matrix C_b^n at time *t* can be expressed as

$$C_b^n = C_r^n C_b^r \quad (1)$$

Where C_r^n is the transformation matrix from the rotational IMU frame to the local level frame, C_b^r is the transformation matrix from the body frame to rotational IMU frame, and we have

$$C_b^r = \begin{bmatrix} \cos(\omega_r t) & \sin(\omega_r t) & 0 \\ -\sin(\omega_r t) & \cos(\omega_r t) & 0 \\ 0 & 0 & 1 \end{bmatrix} \quad (2)$$

Where ω_r denotes the rotating angular velocity.

Consequently, the error model for SRINS is shown as follows:

$$\begin{cases} \dot{\phi}^n = -\delta\omega_{in}^n \times \phi^n + \delta\omega_{in}^n - C_b^n \varepsilon \\ \delta\dot{V}^n = f^n \times \phi^n - (2\omega_{ie}^n + \omega_{en}^n) \times \delta V^n \\ \qquad - (2\delta\omega_{ie}^n + \delta\omega_{en}^n) \times V^n + C_b^n \nabla \\ \delta\dot{\varphi} = \delta V_y / R_m \\ \delta\dot{\lambda} = \delta V_x \sec\varphi / R_n \end{cases} \quad (3)$$

Where δV and ϕ^n denote the velocity error and attitude error, respectively; $\delta\varphi$ and $\delta\lambda$ denote the latitude error and longitude error, respectively; φ is the latitude; ω_{ie}^n denote the angular velocity of earth and $\delta\omega_{ie}^n$ is its error; ω_{en}^n and $\delta\omega_{en}^n$ denote the angle velocity of motion in the navigation frame relative to earth frame and its error; ε and ∇ denote the biases of gyroscopes and accelerometers, respectively; R_m is the radius of Meridian, R_n is the radius of Prime vertical; f^n is the specific force in navigation frame.

In order to reduce the impact on system performance by the scaled factors of inertia components, the reciprocation rotation scheme is chosen. As shown in Fig. 1, during each rotational cycle, the inertial measurement unit (IMU) rotates 360 degrees in the clockwise direction stops for a time T_h; then, IMU rotates 360 degrees in the counter-clockwise direction and stops for a time T_h.

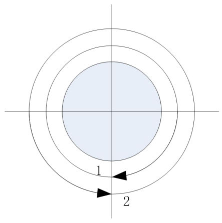

Fig. 1: IMU single-axis rotation scheme

2.2 Level Damping Network of SINS

The value of gyroscope drift in high-precision SRINS is extremely small commonly about $0.003\,^\circ/\mathrm{h}$. Therefore, the estimation of gyroscope drift may last for 5.5 hours or more [6]. On the other hand, error properties of an INS, there are three kinds of dominant oscillations: Schuler oscillation, Foucault oscillation and earth oscillation, especially Schuler oscillation is of a cycle 84.4 minutes. When almost 6-hours comprehensive calibration is implemented, the estimatation errors of an INS would exhibit Schuler oscillations if an INS has been operating without damping, and the gyroscope drifts cannot be estimated effectively.

In order to eliminate these oscillations for calibration, the level damping network is adopted. The velocity measured by Doppler log is propagated to damp Schuler oscillations as well as the Foucault oscillations.

By [7], the transfer functions of level damping network could be expressed as

$$H_X(s) = H_Y(s) = \frac{(s + w_1)(s + w_4)}{(s + w_2)(s + w_3)} \quad (4)$$

Where $H_X(s)$ and $H_Y(s)$ are the transfer functions, $w_1 = 8.5 \times 10^{-4}$, $w_2 = 8.0 \times 10^{-3}$, $w_3 = 1.0 \times 10^{-2}$, $w_4 = 9.412 \times 10^{-2}$.

For the convenience of calculation by computer, a set of intermediate variables are introduced. The control equations for the level damping INS can be written as

$$\begin{cases} \dot{u}_1 = (w_4 - w_3)(V_y - K_1 V_{ry}) - w_4 u_1, \\ \dot{u}_2 = (w_2 - w_3)(V_y - K_1 V_{ry} + u_1) - w_3 u_2 \\ \dot{u}_3 = (w_4 - w_3)(V_x - K_1 V_{rx}) - w_3 u_3 \\ \dot{u}_4 = (w_1 - w_2)(V_x - K_1 V_{rx} + u_3) - w_2 u_4 \end{cases} \quad (5)$$

Where u_1, u_2, u_3, u_4, K_1 are the control variables refer to the level damping network; V_{rx}, V_{ry} are the velocities measured by Doppler log.

3 Filter Design for Calibration

3.1 States of Filter

On the assumption that the rotation is around azimuth axis, the gyroscope drift ε_{bz}^b is the estimated value which is desired in the filtering for compensation. The size of the state vector is of dimension 16 chosen as follows:

$$X = [\phi_x \quad \phi_y \quad \phi_z \quad \delta V_x \quad \delta V_y \quad \delta\varphi \quad \delta\lambda \quad \varepsilon_x^b \quad \varepsilon_y^b \quad \varepsilon_z^b \quad \nabla_x^b \quad \nabla_y^b \quad u_1 \quad u_2 \quad u_3 \quad u_4]^T \quad (6)$$

3.2 State Equation

According to the error equations of SRINS from equations (3), (5) and (6), the system state equation is obtained as

$$\dot{X} = FX + W \quad (7)$$

Where F denotes linearized systems dynamics matrix , the nonzero terms in F are

$F(1,2) = \omega_{ie}\sin(\varphi) + V_x/(R_n \tan(\varphi))$,

$F(1,3) = -(\omega_{ie}\cos(\varphi) + V_x/R_n)$, $F(1,5) = -1/R_m$,

$F(1,8) = C_b^n(1,1)$, $F(1,9) = C_b^n(1,2)$, $F(1,10) = C_b^n(1,3)$,

$F(2,1) = -(\omega_{ie}\sin(\varphi) + V_x/(R_n\tan(\varphi)))$, $F(2,3) = -V_y/R_m$,

$F(2,4) = 1/R_n$, $F(2,6) = -\omega_{ie}\sin(\varphi)$, $F(2,8) = C_b^n(2,1)$,

$F(2,9) = C_b^n(2,2)$, $F(3,1) = \omega_{ie}\cos(\varphi) + V_x/R_n$,

$F(2,10) = C_b^n(2,3)$, $F(3,2) = V_y/R_m$, $F(3,4) = \tan(\varphi)/R_n$,

$F(3,6) = \omega_{ie}\cos(\varphi) + V_x/(R_n\cos^2(\varphi))$, $F(3,8) = C_b^n(3,1)$,

$F(3,9) = C_b^n(3,2)$, $F(3,10) = C_b^n(3,3)$, $F(4,2) = -g$

$F(4,3) = f_y^n$, $F(4,5) = 2\omega_{ie}\sin(phi) + V_x/(R_n\tan(\varphi))$,

$F(4,4) = V_y/(R_n\tan(\varphi))$, $F(5,1) = g$,

$F(4,6) = 2\omega_{ie}V_y\cos(\varphi) + V_xV_y/(R_n\cos^2(\varphi))$, $F(5,3) = -f_x^n$,

$F(5,4) = -(2\omega_{ie}\sin(\varphi) + 2V_x/(R_n\tan(\varphi)))$, $F(6,5) = 1/R_m$

$F(5,6) = -(2\omega_{ie}V_x\cos(\varphi) + V_x^2/(R_n\cos^2(\varphi)))$,

$F(7,4) = 1/(R_n\cos(\varphi))$, $F(7,6) = V_x\tan(\varphi)/(R_n\cos(\varphi))$,

$F(6,11) = 1/R_m$, $F(6,12) = 1/R_m$, $F(7,13) = 1/(R_n\cos(\varphi))$,

$F(7,14) = 1/(R_n\cos(\varphi))$, $F(1,11) = -1/R_m$, $F(1,12) = -1/R_m$,

$F(2,13) = 1/R_n$, $F(2,14) = 1/R_n$, $F(3,13) = \tan(\varphi)/R_n$,

$F(3,14) = \tan(\varphi)/R_n$, $F(6,11) = 1/R_m$,

$F(7,13) = 1/(R_n\cos(\varphi))$,

$F(6,12) = 1/R_m$, $F(7,14) = 1/(R_n\cos(\varphi))$, $F(11,11) = -w_3$

$F(11,5) = w_4 - w_3$, $F(12,5) = w_1 - w_2$, $F(12,11) = w_1 - w_2$,

$F(12,12) = -w_2$, $F(13,4) = w_4 - w_3$, $F(13,13) = -w_3$,

$F(14,4) = w_1 - w_2$, $F(14,13) = w_1 - w_2$, $F(14,14) = -w_2$,

$F(16,5) = 1$, $F(16,11) = 1$, $F(16,12) = 1$, $F(16,15) = -1$;

B, C, D and E are the parameters of the damping network; g denotes the local gravity; f_x^n, f_y^n, f_z^n denote the projections of f^n in the local level coordinate; the W denotes system white noise.

3.3 Measurement Equation

Because the errors of DGPS are not accumulated over time, the high-precision velocity and position provided by DGPS are usually chosen as the reference information for an INS. For the velocity and position matching method, the measurement equations of calibration can be written as

$$Z = \begin{bmatrix} V_x^{INS} - V_x^{DGPS} \\ V_y^{INS} - V_y^{DGPS} \\ \hline P_x^{INS} - P_x^{DGPS} \\ P_y^{INS} - P_y^{DGPS} \end{bmatrix} = HX + V \tag{8}$$

Where V is the measurement white noise, H is termed as an observation operator, and $H = \left[\begin{array}{c|c|c|c} 0_{2\times3} & I_{2\times2} & 0_{2\times2} & 0_{2\times6} \\ \hline 0_{2\times3} & 0_{2\times2} & I_{2\times2} & 0_{2\times6} \end{array}\right]$.

3.4 Kalman Filtering Algorithm

After the dicretization of equation (1), the discretized system equations are

$$\begin{cases} X_k = \Phi_{k,k-1}X_{k-1} + W_{k-1} \\ Z_k = HX_k + V_k \end{cases} \tag{9}$$

Then the standard discrete Kalman filter algorithm is implemented for recursive calculation. The Kalman filtering process can be expressed as

1）Prediction

$$\begin{cases} \hat{X}_{k,k-1}^f = \Phi_{k,k-1}\hat{X}_{k-1}^f \\ P_{k,k-1}^f = \Phi_{k,k-1}P_{k-1}^f\Phi_{k,k-1}^T + Q_{k-1} \end{cases} \tag{10}$$

Where k is the time step $k = 1, 2, \ldots, N$, N is the total calculating steps and is related to the available N measurements.

2）Update

$$\begin{cases} K_k^f = P_{k,k-1}^f H^T [H_k P_{k,k-1}^f H^T + R]^{-1} \\ \hat{X}_k^f = \hat{X}_{k,k-1}^f + K_k^f [Z_k - H\hat{X}_{k,k-1}^f] \\ P_k^f = [I - K_k^f H] P_{k,k-1}^f [I - K_k^f H_k]^T + K_k^f R [K_k^f]^T \end{cases} \tag{11}$$

The output of filter is $\hat{X}_N^f$.

According to the system model above, the comprehensive calibration approach for SRINS is shown as Fig. 2.

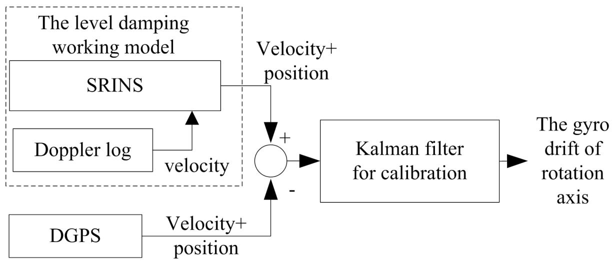

Fig. 2: The basic diagram of comprehensive calibration for SRINS

4 Observability Analysis

The method of observability analysis on the state space model could effectively predict the potential optimality performance criteria for the designed Kalman filter before its implementation. If the state can be observed, the estimation performance of this state would be excellent; if the state cannot be observed, this state might not be estimated effectively. It is of value for the calibration of SRINS in which six or more hours are required during the filtering process. The prospective performance for the estimated gyroscope drift along rotational axis could be predicted by giving out the observability degree.

In the real operating environment, the parameters of SINS are varying over time. Therefore, the system dynamics model is non-stationary. The theory of piece-wise constant system can be a valid method to analyze the observability of this system. In this method, when the carrier motion has not changed, the conventional system total observability matrix (TOM) is replaced by a stripped observability matrix (SOM). Then, the obtained SOM is disposed by singular value decomposition to compute the singular value of each state. The obtained singular value could serve as a kind of quantitative description for system observability. When the singular value of state is greater than 0 as well as very close to 1, this state could be well estimated; when the value is extremely near 0, such as being less than 0.00001, this state would be considered as unobservable and could not be estimated by using this scheme [8].

4.1 Observability Matrix of System

Assuming that the carrier maintains uniform motion state during the process of comprehensive calibration, the TOM of system can be represented by a single SOM. The SOM can be expressed as

$$Q = [H \quad HF \quad \cdots \quad HF^{n-1}]^T \tag{12}$$

Implementing the singular value decomposition of equation (12), we obtain

$$Q = U\Sigma D^T \tag{13}$$

Where $\Sigma = \mathrm{diag}\{S,0\}$, $S = \mathrm{diag}\{\sigma_1,\sigma_2,\ldots,\sigma_k\}$; $\sigma_1,\sigma_2,\ldots,\sigma_k$ are the singular values of the observable states with a descending rank order of these values. The dimension m of SOM is equivalent to the observable states, which is indicated as

$$m = \mathrm{rank}(\Sigma) \tag{13}$$

4.2 Results of Observability Analysis

The error parameters of sensors involved are setting as follows. The drifts of all three gyroscopes are 0.003 $°/h$, their angle random walks are 0.0005 $°/\sqrt{h}$, the scale factor error is 10 ppm; the installation error is 2"; the biases of accelerometers are 20 μg , their measurement noises are 1 μg . The measurement noise of DGPS velocity and position are 0.01m/s and 10m, respectively.The carrier is in the uniform motion state at the speed of 1m/s.

Executing the observability analysis based on singular value decomposition, we gained the results as follows:

The rank of SOM is nine, which means that there are nine states could be observed and estimated. The nine observable states and their singular values are summarized in Table 1.

Table 1. The observability analysis results of system

State	Singular value
ϕ_y	52.487201395665203
ε_{bx}^{b}	9.803897443003379
ϕ_x	9.803896981377633
ε_{by}^{b}	6.887730926542787
$\delta\lambda$	1.000000000000000
δV_y	1.000000000000000
$\delta\varphi$	0.999999998779838
δV_x	0.994784375323066
ε_{bz}^{b}	0.000529405155275

The histograms of observable states are shown in Fig. 3.

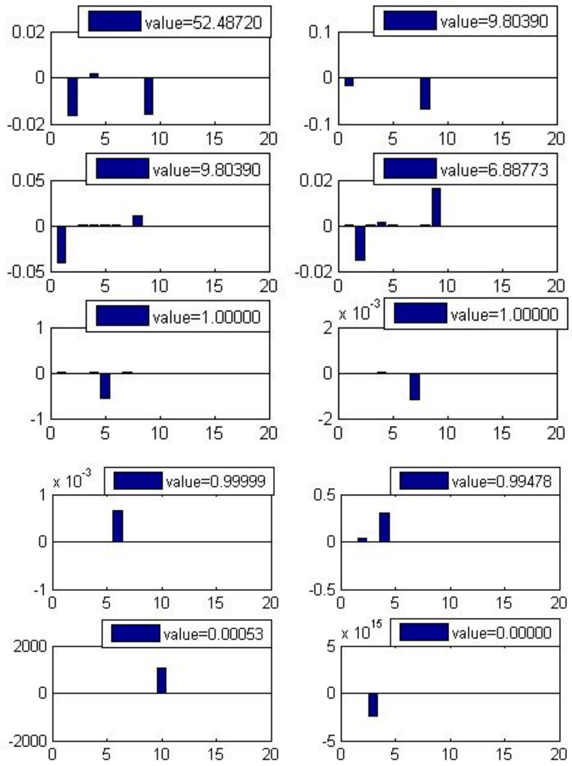

Fig.3: The histograms of observable states

From Table 1, the singular value of rotation-axis gyroscope drift ε_{bz}^{b} is just slightly larger than 0.00001, which means that the observability of ε_{bz}^{b} is not good enough. The dynamics injected in this axis is not large enough for the sensor to excite its errors. And ε_{bz}^{b} can only be estimated through quite longe time observation and filtering. Therefore, many hours matching filtering estimation are necessary for effectively calibration of SRINS. This requires that the SRINS must operate on the damping model to restrain the influence of the Schuler oscillation error on the drift estimation [9].

5 Simulation

5.1 Calibration without Maneuvering

Simulations are conducted when the SRINS is working on the level damping mode. The simulation time is 30 hours. The error curves for SRINS are shown in Fig. 4.

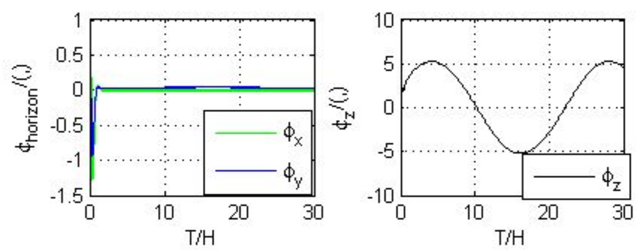

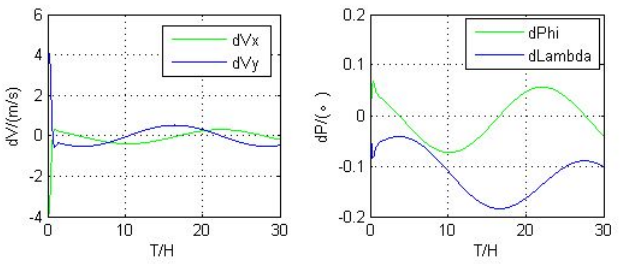

Fig.4: The error curves for SRINS working on the level damping mode

Figure 4 shows that the Schuler oscillation of SRINS is efficiently damped by utilizing the level damping network. The period of residual earth oscillation is much greater than the period of Schuler oscillation. Thus, the residual earth oscillation can be ignored as slowly-varying variables. SRINS working on the level damping mode could guarantee the validity of this scheme.

Discrete Kalman filtering algorithm is utilized for the comprehensive calibration of SRINS. After 24-hours of operation, 10-hours filtering process is implemented. The carrier motion is the same as that mentioned in section 4.2. The estimated gyroscope drifts are shown in Fig. 5 and Fig. 6.

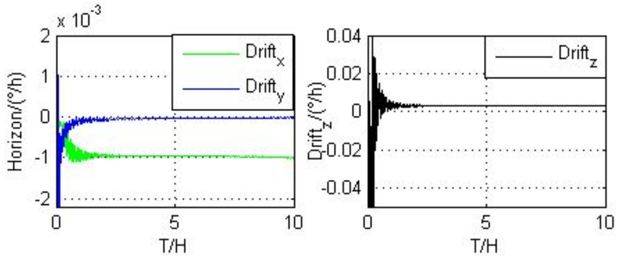

Fig.5: The estimate curves of gyroscope drifts

In Fig. 5, the obtained gyroscope drifts ε_{bx}^{b} and ε_{by}^{b} are the equivalent drifts after being modulated, which have less magnitude than the real value. This indicates that the rotational modulation method can effectively improve the performance of INS without substituting any inertial sensor. The estimate curve of ε_{bz}^{b} is convergent.

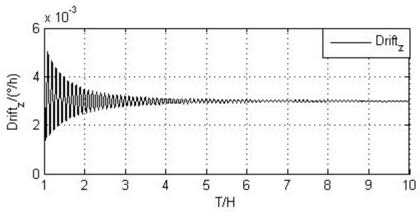

Fig.6: The detailed estimate curve of ε_{bz}^{b}

Fig. 6 shows the local details of the estimate curve of ε_{bz}^{b}. After about 6 hours of filtering, the estimates of ε_{bz}^{b} converge to a stable value. Therefore, the gyroscope drift of azimuth axis can be accurately estimated by using the proposed scheme.

5.2 Calibration with Linear Accelerated Motion

Linear accelerated motion is usually introduced to improve the estimated performance for the variables about the azimuth axis such as the azimuth angle. For the coupling effect between the azimuth angle and the azimuth drift, the effect of linearly accelerated motion on the calibration is studied in the following.

For the level damping working mode, the introduced accelerated motion would cause a short-time overshoot on the error curve [10]. The linearly accelerated motions are respectively introduced in two-time calibration processes.

Condition 1: Introduce the linearly accelerated motion on the steady state period of calibration.

Assuming the carrier is motioning towards the east with the velocity of 1 m/s. After 4.5 hours of calibration filtering, the eastward linear maneuvering is implemented with the acceleration of 0.1 m/s^2 lasting for 20 seconds. The obtained estimation curves of this situation are shown in Fig. 7.

From Fig. 7, the eastward linearly accelerated motion during the steady state period would results in an obvious overshoot vibrations on all drift estimated curves. The steady state estimates of horizontal drifts are varied with large magnitudes. Therefore, the estimation precisions of them are degraded due to the maneuvering. However, the azimuth drift curve has not been impacted greatly. There is only a modest overshoot appearing in the curve. Meanwhile, the steady state value of the azimuth drift estimate has not been influenced by this maneuvering.

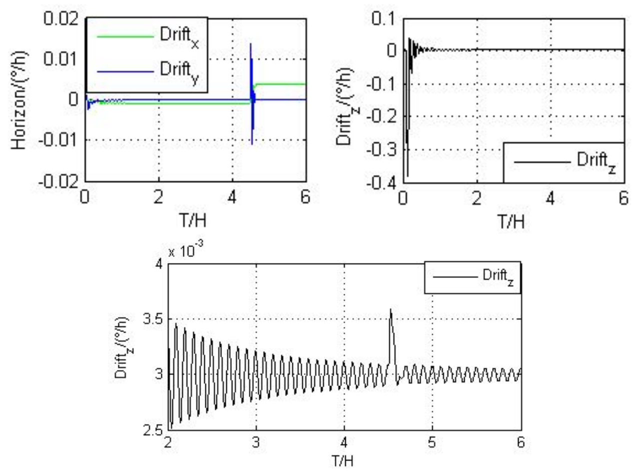

Fig.7: The estimated curves of gyroscope drifts with maneuvering in the steady state period

Condition 2: Introduce the linearly accelerated motion on the initial period of calibration.

The same maneuvering being illustrated above is executed after 1.5 hours of filtering. The estimate results are shown in Fig. 8.

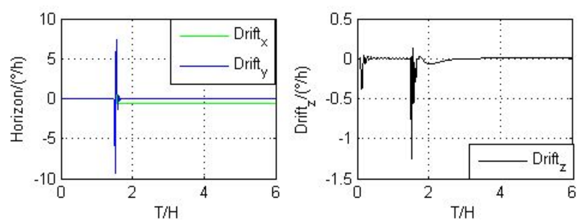

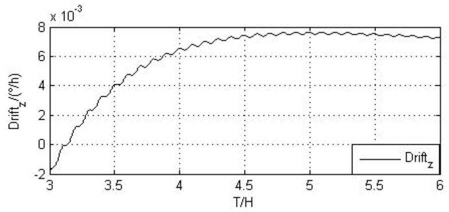

Fig.8: The estimate curves of gyroscope drifts with maneuvering in the initial period

From Fig. 8, the filtering results appear much larger overshoot when the maneuvering is carried out during the initial period than the steady state period. All gyroscope drifts cannot be precisely estimated due to the large overshoots on the attitude errors. The attitude errors are shown in Fig. 9. The errors of ϕ_y and ϕ_z are too large for normal filtering calculation. Hence, this attitude error has undermined the assumption of small angle error. After maneuvering, the estimate of azimuth drift exhibits obvious steady state error. More time is required for the convergence of azimuth drift curve.

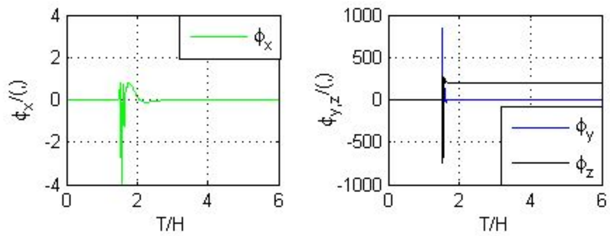

Fig.9: The estimate curves of attitude errors

By the analysis above, it can be seen that the linearly accelerated motion implemented in different periods of calibration have different influences on the estimate results. In the initial period of calibration, the carrier motion should be restricted to confirm the filtering precision. And in the steady state period, the maneuvering could be considered to accelerate the convergence of the azimuth drift without a cost of accuracy.

6 Conclusions

In this paper, the comprehensive calibration for SRINS were studied. Considering the error propagating characteristic of SRINS, a comprehensive calibration scheme based on the level damping working mode has been presented. The velocity and position from DGPS are imported as a reference information. By using the Kalman filter, the gyroscope drift of rotational axis could be accurately estimated. The validity of this approach has been confirmed by observability analysis method and simulations. Finally, the impacts of carrier maneuvering on the calibration are analyzed.

References

[1] D. Titterton, J.Weston, *Strapdown Inertial Navigation Technology*. Second Edition. United Kingdom: Institution of Electrical Engineers, 2004, chapter 12.

[2] E. Levinson, J. Ter Horst and M. Willcocks, The next generation marine inertial navigator is here now, in *IEEE/ION Position Location and Navigation Symposium,* 1994: 121-127.

[3] J. Cheng , B. Wang and D. Chen, Error Analyzing Method for Rotation Inertial Navigation System Based on Fourier Transform, *Applied Mechanics and Materials*, 336: 982-987, 2013.

[4] P. Feng, K. Li and W. Wang, New comprehensive calibration method of carrier-based inertial navigation system, *Journal of Chinese Inertial Technology*, 19(4): 427-437, 2011.

[5] C. Wang, H. Zhu and D. Gao, Comprehensive calibration of rotation axis gyro constant bias for single-axial rotation of INS, *Journal of Chinese Inertial Technology*, 20(04): 421-424,2012.

[6] Z. Zhou, H. Xu and L. Wu, Analysis and estimation for azimuth gyro drift of single-axis rotation SINS, *Journal of Chinese Inertial Technology*, 21(01): 31-36, 2013.

[7] D. Huang, L. Cheng. *Inertial Navigation System*, Harbin: Harbin Engineering University Press, 1999, chapter 5.

[8] L. Zhao, L. Li and M. Sun, Analysis on observability of SINS multi-position alignment based on singular value decomposition, *Journal of Chinese Inertial Technology*, 16(5): 523-528, 2008.

[9] Y. Liu, X. Zhen and Q. Li, Integrated navigation method of strapdown inertial navigation system under damping condition, *Control Technology of Tactical Missile*, 26(3): 13-16, 2009.

[10] J. Cheng, L. Zhao and J. Song, Application of auto-compensation technology to the switches of INS states, *Journal of Harbin Engineering University*, 26(6): 744-748, 2005.